1 **Large particulate nitrate formation from N₂O₅ uptake in a**

2 **chemically reactive layer aloft during wintertime in Beijing.**

3 *Haichao Wang[1], Keding Lu[1]*, Xiaorui Chen[1], Qindan Zhu[1,#], Zhijun Wu[1], Yusheng*

4 *Wu[1], Kang Sun[2]*

5 [1]State Key Joint Laboratory of Environmental Simulation and Pollution Control, College of

6 Environmental Sciences and Engineering, Peking University, Beijing, China

7 [2]China National Environmental Monitoring Centre, Beijing, China

8 [#]Now at the Department of Chemistry, University of California, Berkeley, CA 94720, USA

10 *Correspondence to: Keding Lu (k.lu@pku.edu.cn)*

12 **Abstract.**

13 Particulate nitrate (pNO_3^-) is a dominant component of secondary aerosols in urban

14 areas. Therefore, it is critical to explore its formation mechanism to assist with the

15 planning of haze abatement strategies. Simultaneous ground-based and tower-based

16 measurements were conducted during a winter heavy haze episode in urban Beijing,

17 China. We found pNO_3^- formation via N_2O_5 heterogeneous uptake was negligible at

18 ground level, due to the presence of high NO concentrations limiting the production

19 of N_2O_5. In contrast, the contribution from N_2O_5 uptake was larger at higher altitudes

20 (e.g., > 150 m), which was supported by the observed large total oxidant ($NO_2 + O_3$)

21 missing aloft compared with ground level. The nighttime integrated production

22 potential of pNO_3^- for the higher altitude air mass overhead urban Beijing was

23 estimated to be 50 μg m⁻³, and enhanced the surface pNO_3^- significantly with 28 μg

24 m⁻³ after nocturnal boundary layer broken in the next morning. In this case, the

25 oxidation of NO_X to nitrate was maximized once N_2O_5 uptake coefficient over 0.0017,

26 since N_2O_5 uptake dominated the fate of NO_3 and N_2O_5 with the presence of large

27 aerosol surface concentrations. These results highlight that pNO_3^- formation via N_2O_5

28 heterogeneous hydrolysis at higher altitude air masses aloft could be an important

29 source for haze formation in the urban airshed during wintertime. Accurately

30 describing the formation and development of reactive air masses aloft is a critical task

31 for improving current chemical transport models.

32

1. Introduction

34 Winter particulate matters (PM) pollution events occur frequently in China, and have

35 drawn widespread and sustained attention in recent years (Guo et al., 2014; Zhang et

36 al., 2015; Huang et al., 2014). PM pollution reduced visibility (Lei and Wuebbles,

37 2013) and had harmful effects on public health (Cao et al., 2012). Particulate nitrate

38 (pNO_3^-) is an important component of secondary inorganic aerosols, and contributed

39 to 15–40% of the $PM_{2.5}$ mass concentration in China (Sun et al., 2013, 2015a, 2015b;

40 Chen et al., 2015; Zheng et al., 2015; Wen et al., 2015). The main atmospheric

41 pathways of nitrate formation are (1) the reaction of OH with NO_2 and (2) N_2O_5

42 heterogeneous hydrolysis (Seinfeld and Pandis, 2006). The first reaction (OH + NO_2)

43 was a daytime pathway since OH is severely limited at night, and N_2O_5 uptake was

44 refer to a nighttime pathway as NO_3 and N_2O_5 is easily photo-labile.

45 Nitrate formation via N_2O_5 heterogeneous hydrolysis was proved efficient by

46 ground based observation in summer in North China (H.C. Wang et al., 2017b; Z.

47 Wang et al., 2017), which is comparable with or even high than the daytime formation.

48 Several model studies showed N_2O_5 hydrolysis is responsible for nocturnal pNO_3^-

49 enhancement in Beijing (Pathak et al., 2009, 2011; H.C. Wang et al., 2017a). Although

50 the pNO_3^- formation via N_2O_5 uptake is significant in summertime, the importance of

51 this pathway in wintertime was not well characterized. As there are many differences

52 of N_2O_5 chemistry between winter and summer. First, as the key precursor of NO_3 and

53 N_2O_5, O_3 level are much lower in winter than in summer due to short daytime length

54 and weak solar radiation. Second, colder temperatures and high NO_2 levels favor

55 partitioning towards N_2O_5. Third, nighttime lasts much longer in winter, making N_2O_5

56 heterogeneous hydrolysis potentially more important in pNO_3^- formation. Finally,

N$_2$O$_5$ uptake coefficient, the most important parameter in N$_2$O$_5$ heterogeneous hydrolysis, is likely very different from that in summer. Since the particle characteristics and meteorological conditions (e.g. organic compounds, particle nitrate, liquid water contents, solubility, viscosity and relative humidity) are different in summer and winter (Chen et al., 2015; Zhang et al., 2007). These differences would result in the N$_2$O$_5$ uptake coefficient has large variation (Wahner et al., 1998; Mentel et al., 1999; Kane et al., 2001; Hallquist et al., 2003; Thornton et al., 2003; Bertram and Thornton, 2009; Grzinic et al., 2015; Wagner et al., 2013).

In addition to seasonal differences, previous studies have also shown a potential altitude dependence in pNO$_3^-$ production. In the evening, vertical mixing is strong suppressed in nocturnal boundary layer (NBL) due to the reduction of sunlight diminishes the heating of the earth's surface, leading to vertical layer occur with NO$_3$ and N$_2$O$_5$ gradient (Brown et al., 2007), as well as the particle compounds percentage and size distribution (Ferrero et al., 2010; 2012). On nights when NO$_3$ radical production in the surface layer is negligible due to high NO emissions, N$_2$O$_5$ uptake may still be active aloft without NO titration (Pusede et al., 2016; Baasandorj et al., 2017). The N$_2$O$_5$ uptake aloft leads to elevated pNO$_3^-$ formed in the upper layer with effective NO$_X$ removal (Watson et al .,2002; S.G. Brown et al., 2006; Lurmann et al., 2006), which was reported with field observations at a high altitude site in Kleiner Feldberg, Germany (Crowley et al., 2010a), London British Telecommunications tower, UK (Benton et al., 2010), Boulder Atmospheric Observatory (BAO) tower in Colorado, USA (Wagner et al., 2013) and so on. Model studies also proposed nitrate formation varied in different height (Kim et al., 2014; Ying, 2011; Su et al., 2017). The mass fraction and concentration of pNO$_3^-$ in Beijing was reported higher aloft (260 m) than at the ground in Beijing (Chan et al., 2005; Sun et al., 2015b), and they explained the favorable gas−particle partitioning aloft under lower temperature conditions.

To explore the possible sources of pNO$_3^-$ and the dependence of altitude in wintertime, we conducted vertical profile measurements of NO, NO$_2$, and O$_3$ with a tower platform in combination with simultaneous ground measurements of these

87 parameters in urban Beijing. A box model was used to investigate the reaction rate of

88 N_2O_5 heterogeneous hydrolysis and impact on pNO_3^- formation at different altitudes

89 during a heavy haze episode over urban Beijing. Additionally, the dependence of

90 pNO_3^- formation on the N_2O_5 uptake coefficient was probed.

91

92 **2. Methods**

93 **2.1 Field measurement**

94 Ground measurement (15 m above the ground) was carried out in the campus of

95 Peking University (PKU, 39°59'21"N, 116°18'25"E) in Beijing, China. The location

96 of the PKU site was shown in Fig. 1, as well as the vertical measurement site (IAP,

97 introduced below). At PKU site, dry-state mass concentration of $PM_{2.5}$ was measured

98 by a TEOM 1400A analyzer. NOx was measured by chemiluminescence analyzer

99 (Thermo Scientific, TE-42i-TR) and O_3 was measured by a UV photometric O_3

100 analyzer (Thermo Scientific, TE-49i). Dry state particle number and size distribution

101 (PNSD) was measured from 0.01 to 0.6 μm with a Scanning Mobility Particle Sizer

102 (SMPS, TSI Inc. 3010). These parameters were listed in Table S1. The data were

103 collected from December 16 to 22, 2016. Additionally, relative humidity (RH),

104 temperature (T), wind direction and speed were available during the measurement

105 period.

106 Vertical profile measurements were conducted from December 18 to 20, 2016 at the

107 tower-based platform (maximum height: 325 m) on the campus of the Institute of

108 Atmospheric Physics, Chinese Academy of Sciences (IAP, 39°58'28"N, 116°22'16"E),

109 during a heavy PM pollution episode. The IAP site is just with 4 km distance from the

110 PKU site. The measurement instruments were installed on board a movable cabin on

111 the tower. The ambient NOx and O_3 concentrations were measured with two

112 low-power, light-weight instruments (Model 405 nm and Model 106-L; 2B

113 Technologies, USA). The Model 405 nm instrument measures NO_2 directly based on

114 the absorbance at 405 nm, and NO is measured by adding excess O_3 (conversion

115 efficiency ~100%). The limit of detection of both NO and NO_2 is 1 part per billion

116   volume (ppbv), with an accuracy of 2 ppbv or 2% of the reading, and the time

117   resolution is 10 s. The Model 106-L instrument measures O_3 based on the absorbance

118   at 254 nm with a precision of 1 ppbv or 2% of the reading and a limit of detection of 3

119   ppbv. Height information was retrieved from the observed atmospheric pressure

120   measured by Model 405 nm instrument. The cabin ascended and descended at a rate

121   of 10 m min^{-1}, with a height limit of 260 m at daytime and 240 m at night. The cabin

122   stopped after reaching the peak and parameters were measured continually for the last

123   10 min of each cycle. One vertical cycle lasted for approximately 1 h. We measured

124   two cycles per day, one in the morning and the other in the evening.

125

126   **2.2 Box model simulation**

127   A box model was used to model the NO_3 and N_2O_5 mixing ratios and the nitrate

128   formation potential in vertical scale at IAP site. A simple chemical mechanism (see

129   R1-R5) is used to model the nighttime NO_3 and N_2O_5 chemistry in NO free air masses,

130   and the physical mixing, dilution, deposition, or interruption during the transport of

131   the air mass were not considered. Here f represents the $ClNO_2$ yield from N_2O_5 uptake.

132   Homogeneous hydrolysis of N_2O_5 and NO_3 heterogeneous are neglected in this

133   analysis because there is little absolute humidity and extremely low NO_3

134   concentration during wintertime (Brown and Stutz, 2012). The corresponding rate

135   constants of R1- R3 are those reported by Sander et al., (2011).

136   (R1) $NO_2 + O_3 \;\rightarrow\; NO_3 + O_2$

137   (R2) $NO_2 + NO_3 + M \;\rightarrow\; N_2O_5 + M$

138   (R3) $N_2O_5 + M \;\rightarrow\; NO_2 + NO_3 + M$

139   (R4) $NO_3 + VOCs \;\rightarrow\; Products$

140   (R5) $N_2O_5 + (H_2O \text{ or } Cl^-) \rightarrow (2\text{-}f) NO_3^- + f\,ClNO_2$
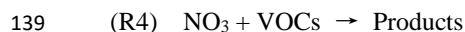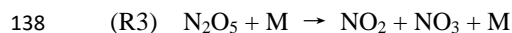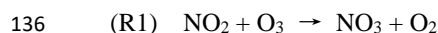
141   Following the work of Wagner et al., (2013), the box model can be solved by four

142   equations (Eq. 1-4). In the framework, O_3 only losses via the reaction of $NO_2 + O_3$ and

143   the change of the O_3 concentration can express as Eq. 1. Since the ratio of N_2O_5 to

144   NO_3 was calculated to be larger than 150:1 in a typical urban region in wintertime

145   (NO_2 = 15 ppbv, nighttime temperature = 0 ℃), N_2O_5 is proposed to be dominate the

146   NO_3 loss, than means two molecules of NO_2 lost (convert to nitrate or $ClNO_2$) for one

147   molecule NO_3 formed (Eq. 2). In the model we need to know the mixing ratio of NO_2

148   and O_3 at time zero (here set to sunset). According to Eq. 1 and Eq. 2, the NO_2 (t=0)

149   and O_3 (t=0) concentration can derived from the duration time and the vertical

150   measured NO_2 and O_3 at each height. Assuming the equilibrium between NO_3 and

151   N_2O_5 is maintained after a time period, the sum concentration of NO_3 and N_2O_5 can

152   be described by Eq. 3. Using the temperature dependent equilibrium rate constant (k_{eq})

153   and the modeled NO_2 at a certain time, Eq. 4 can be used to determine the ratio of

154   N_2O_5 and NO_3. Combined, Eq. 1-4 allow for the calculation of N_2O_5 concentrations,

155   given a constant of NO_3 and N_2O_5 rate constant (k_{NO3} and k_{N2O5}). Modeled N_2O_5

156   concentrations and given k_{N2O5} are then used to estimate pNO_3^- formation, here the

157   HNO_3 produced in R4 is not accounted, as a large part of the products are organic

158   nitrates (Brown and Stutz, 2012). Here k_{NO3} and k_{N2O5} denotes the pseudo first order

159   reaction rate constant of the total NO_3 reactivity caused by ambient volatile organic

160   compounds (VOCs) and N_2O_5 heterogeneous uptake, respectively. k_{N2O5} is given in

161   Eq. 5. S_a is aerosol surface area, C is the mean molecular speed of N_2O_5, and γ_{N2O5} is

162   N_2O_5 uptake coefficient. The model is run from sunset to sunrise, where the length of

163   night was about 14.5 h.

164   (Eq. 1) $\dfrac{d\,[O_3]}{dt} = -k_{NO2+O3}[O_3][NO_2]$

165   (Eq. 2) $\dfrac{d\,[NO_2]}{dt} = -2 \times k_{NO2+O3}[O_3][NO_2]$

166   (Eq. 3) $\dfrac{d\,[NO_3+N_2O_5]}{dt} = k_{NO2+O3}[O_3][NO_2] - k_{N2O5}[N_2O_5] - k_{NO3}[NO_3]$

167   (Eq. 4) $\dfrac{[N_2O_5]}{[NO_3]} = k_{eq}[NO_2]$

168   (Eq. 5) $k_{N2O5} = \dfrac{C \times S_a \times \gamma_{N2O5}}{4}$

169   Dry-state S_a at PKU site was calculated based on the PNSD measurement, which

170   was corrected to ambient (wet) S_a for particle hygroscopicity by a growth factor (Liu

171   et al., 2013). The uncertainty of the wet S_a was estimated to be ~30%, which was

172   associated from the error from dry PNSD measurement (~20%) and the growth factor

173   (~20%). Nighttime averaged S_a on the night of December 19 is about 3000 μm^2 cm^{-3}.

174   PM measurements by National Monitoring Sites proved this heavy haze pollution

175   episode was a typical regional event (Fig. S1). Furthermore, synchronous study on the

176   night of December 19, 2016 shown small variation of vertical particle number

177   concentration, with the boundary layer height below 340 m (Zhong et al., 2017).

178   Therefore, the S_a at PKU site is representative to the urban Beijing conditions and

179   applied in the model is reasonable.

180   N_2O_5 uptake coefficient was regard as the main uncertainty of the N_2O_5 loss, along

181   with the $ClNO_2$ yield lead to the uncertainties in the estimation of particulate nitrate

182   formation (Thornton et al., 2010; Riedel et al., 2013; Wagner et al., 2013; Phillips et

183   al., 2016). Wagner et al., (2013) shows the significant particular nitrate suppression

184   aloft in the wintertime in Denver, USA, with the uptake coefficient of about 0.005

185   when particulate nitrate fraction in the $PM_{2.5}$ mass concentration about 40%.

186   Considered the high particle nitrate content in North China in wintertime is similar to

187   that in Denver (Sun et al., 2013, 2015a; Chen et al., 2015; Zheng et al., 2015; Wen et

188   al., 2015), here we used a constant uptake coefficient of 0.005 as the model initial

189   input in the base case, and the uncertainty of N_2O_5 uptake coefficients will be

190   discussed later. Since the model input of $ClNO_2$ yield only affect the value of

191   produced particulate nitrate concentration, and would not change the modeled N_2O_5

192   concentration, here we set the initial f_{ClNO2} to zero. The impact of $ClNO_2$ yield will be

193   further discussed later.

194   Respect to k_{NO3}, the average value in summertime was estimated to be 0.024 s^{-1} in

195   2006 (H.C. Wang et al., 2017a). While in wintertime, the k_{NO3} should be smaller as

196   the intensity of plant emissions reduced in the lower temperature and weak solar

197   radiation. The model input $k(NO_3)$ was set to an relative moderate value of 0.02 s^{-1}

198   (equivalent to 0.2 ppbv isoprene + 40 pptv monoterpene + 1.0 ppbv cis-2-butene). A

199   series of sensitivity tests were conducted to study the uncertainties to the model

200   simulation, and the detailed test set were listed in Table 1, included the test of N_2O_5

201   uptake coefficient and k_{NO3}. The γ_{N2O5} sensitivity tests were set to a lower limit of

202   0.001 to a upper limit of 0.05, as well as the k_{NO3} set to 0.001, 0.01 and 0.1 s^{-1}.

3. Results and discussion

3.1 Ground-based observations.

A severe winter PM pollution event was captured from the ground observations from December 16 to 22, 2016 in Beijing. Figure 2a shown the mass concentration of $PM_{2.5}$ began to increase on December 16 and reached the maximum value of 480 μg m^{-3} December on 20. A fast PM growth event happened on the night of December 19–20 (colored red in Fig. 2a), the $PM_{2.5}$ mass concentration increased continuously throughout the night, with an overall increment of 100 μg m^{-3}. During the episode, the meteorological condition is featured with high RH (50% ±16%) and low temperature (2 ± 3 °C). The slow surface wind (< 3 m s^{-1}) indicated the atmosphere was static stabilized (Fig. 2c, 2d). The daytime O_3 concentration was low due to high NO emission and weak solar radiation. After sunset, O_3 was rapidly titrated to zero by the elevated NO. The presence of high NO concentrations would have strongly suppressed the concentration of NO_3, and further suppressed N_2O_5 near the ground. Figure 2b depicted large amounts of NO and NO_2 were observed throughout the whole PM pollution episode, suggesting that pNO_3^- production via N_2O_5 uptake was not important near the ground during the winter haze episode.

3.2 Tower observations.

Six vertical measurements of Ox (< 50 m) was consist with that measured at ground level and shown in Fig. S2, confirmed the two sites are comparable at ground level at last. On the night of December 20 (Fig. 3a), the NO_2 and NO from 0-240 m were abundant and conservative around 21:00, with the concentration of 80 ppbv and 100 ppbv, respectively. The O_3 concentrations keep zero during the nighttime (Fig. 3b). The vertical profile on December 20 suggests that at least below 240 m, the N_2O_5 chemistry is also not important like ground level as mentioned above. The case on the night of December 18 is similar to the night of December 20.

The vertical measurement on December 19 did not like those happened on

231   December 18 and 20. Figure 4a shows the vertical profiles around 21:00 on December

232   19 that NO was abundant from the ground to 100 m, then gradually decreased to zero

233   from 100 m to 150 m, and stay zero above 150 m. The observed NO_2 concentration

234   was 85 ± 2 ppbv below 100 m, which gradually decreased from 100 m to 150 m, and

235   was 50 ± 2 ppbv from 150 m to 240 m. The observed O_3 concentrations were below

236   the instrument limit of detection below 150 m (Fig. 4b). Above 150 m, the O_3

237   concentration was 20 ± 2 ppbv, corresponding to the greatly diminished NO

238   concentration. With respect to the total oxidants ($Ox = O_3 + NO_2$), the mixing ratio of

239   Ox was 85 ± 2 ppbv at lower altitudes, while the Ox concentration at higher altitudes

240   was 15 ppbv lower than that at lower altitude (Fig. 4b). The O_X missing at the higher

241   altitude air mass indicated an additionally nocturnal removal of Ox aloft.

242   Figure 5 depicted the vertical measurement at 09:30 on the morning of December

243   20 has similar features with those observed at 21:00 on December 19, and the NBL

244   still not be broken. The O_X missing aloft in the morning increased to 25 ppbv at

245   240–260 m, demonstrated that an additional 25 ppbv of Ox was removed or converted

246   to other compounds at higher altitudes than surface layer on the night of December

247   19-20. Figure S3 shows the vertical profiles of NO, NO_2, O_3 and Ox at ~12:00 on

248   December 18, when the solar radiation is strong enough to drive the trace gas mixing

249   well in vertical direction. NOx and O_3 were observed well mixed indeed, with small

250   variation from ground level to 260 m.

251

3.3 Particulate nitrate formation aloft.

253   N_2O_5 uptake is one of the two most important pathways of the ambient NO_X losses,

254   and is consequently an important pathway of pNO_3^- formation (Wagner et al., 2013;

255   Stutz et al., 2010; Tsai et al., 2014). At higher altitudes (e.g. > 150 m), NO_3 and N_2O_5

256   chemistry can be initiated in the co-presence of high NO_2 and significant O_3 levels.

257   Therefore, N_2O_5 uptake could represent a plausible explanation for the observed O_X

258   missing in the higher-altitude air masses on the night of December 19. To explore this

259   phenomenon, a time-step box model was used to simulate the NO_3 and N_2O_5

260   chemistry based on the observed vertical profiles of NO_2 and O_3 on the night of

261   December 19.

262   In the base case, the modeled N_2O_5 concentration is zero below 150 m, as the high

263   level NO consumed NO_3 formation fast. While the modeled N_2O_5 concentrations at

264   21:00 were in the range of 400-600 parts per trillion volume (pptv) above 150 m (Fig.

265   5a). pNO_3^- accumulation via N_2O_5 heterogeneous hydrolysis from sunset to the

266   measurement time was significant, yielding a maximum of 24 μg m^{-3} within 4.5 hours

267   after sunset (Fig. 5(b)).

268   The box model enabled the analysis of the integrated pNO_3^- and $ClNO_2$ via N_2O_5

269   uptake over the whole night. As shown in Fig. 5c, the modeled integrated pNO_3^- went

270   up to as high as 50 μg m^{-3}. The integrated pNO_3^- at sunrise was equal to the loss of 27

271   ppbv O_X, shows a good agreement with the observed O_X missing aloft at the morning

272   hours. During the nighttime, the formed pNO_3^- aloft via N_2O_5 uptake would lead to

273   the particle nitrate concentration much higher than that in the surface layer, which has

274   been reported many field observations (Watson et al .,2002; S.G. Brown et al., 2006;

275   Lurmann et al., 2006; Ferrero et al., 2012; Sun et al., 2015b). In addition, during the

276   morning time when NBL was broken, the elevated pNO_3^- aloft will vertically mixed

277   and enhanced the PM concentration at surface layer, this phenomenon also been

278   observed in previous studies (Watson et al .,2002; S.G. Brown et al., 2006; Lurmann

279   et al., 2006). In this case, the planetary boundary layer (PBL) height during the

280   daytime is about 340 m on December 20 (Zhong et al., 2017). Assuming that the

281   height of NBL and planetary boundary layer (PBL) are the same, and the air mass was

282   well mixed in the following morning in the PBL. The nighttime N_2O_5 uptake aloft

283   would be enhanced the ground pNO_3^- mass concentration significantly with 28 μg m^{-3}

284   in the morning, which is in good agreement with the observed PM peak in the

285   morning on December 20, with the PM enhancement of ~60 μg m^{-3}. The result

286   demonstrated that the nocturnal N_2O_5 uptake aloft and downward transportation are

287   really importance in understanding the PM growth process.

288

289   **3.4 Sensitivity studies.**

290   Previous studies have emphasized that the N_2O_5 uptake coefficient varies greatly

291   (0.001–0.1) in different ambient conditions (Brown and Stutz, 2012; H.C. Wang et al.,

292   2016), which is the main source of uncertainties in the model. Sensitivity tests

293   illustrate that the modeled N_2O_5 concentration varied from 3 ppbv to 60 pptv when the

294   N_2O_5 uptake coefficients were varied from 0.001 to 0.05 (Fig. 6a), the N_2O_5

295   concentration is very sensitivity to the loss from heterogeneous reaction. Compared

296   with the base case, the accumulated pNO_3^- is evidently lower at $\gamma = 0.001$ with the

297   accumulated pNO_3^- of 44 μg m^{-3}, the low N_2O_5 uptake coefficient condition is

298   corresponding to several kinds of aerosols, such as secondary organic aerosol (Gross

299   et al., 2009), humic acid (Badger et al., 2006)) and certain solid aerosols (Gross et al.,

300   2008). When the N_2O_5 uptake coefficient enlarges from 0.005 to 0.05 (Fig. 6b, c), the

301   integral pNO_3^- almost not change with negligible increasing, indicating that the

302   conversion capacity of N_2O_5 uptake to pNO_3^- was almost maximized at certain $ClNO_2$

303   yield, the convert capacity of NOx to nitrate was not limited by N_2O_5 heterogeneous

304   reaction rate, but the formation of NO_3 by the reaction of NO_2 with O_3.

305   For describing the nocturnal NOx convert capacity to particulate nitrate via N_2O_5

306   uptake coefficient, here we defined the particle nitrate convert efficiency (ε) as Eq. 6.

307   The Δt represents the time duration from time zero at sunset till the ending time at

308   sunrise.

309   (Eq. 6) $\varepsilon = \dfrac{\sum_0^{\Delta t} k_{N2O5}[N_2O_5]}{\sum_0^{\Delta t} 2 \times k_{NO2+O3}[O_3][NO_2]}$

310   In the case, S_a is set to 3000 μm^2 cm^{-3}, the $ClNO_2$ yield is zero and k_{NO3} is 0.02 s^{-1}.

311   Figure 7 shows the dependence of the particle nitrate convert efficiency varied from

312   10^{-5} to 0.1. When γ_{N2O5} is lower than 0.0017, the particle nitrate formation enhanced

313   rapidly with the increasing of N_2O_5 uptake coefficient, here we defined as the γ_{N2O5}

314   sensitive region when $\gamma_{N2O5} < 1.7 \times 10^{-3}$. While $\gamma_{N2O5} \geq 1.7 \times 10^{-3}$ is defined as γ_{N2O5}

315   insensitive region, since the convert efficient is over 90% and not sensitive to the

316   variation of N_2O_5 uptake coefficient. According to Eq. 3 and Eq. 5, higher aerosol

317   surface concentration, higher NOx, lower k_{NO3} and temperature would further

318   enlarging the insensitivity region with lower γ_{N2O5} value, and make the N_2O_5 uptake

319   more easily located in the γ_{N2O5} insensitive region. Here the critical value of the N_2O_5

320   uptake coefficient (1.7×10^{-3}) is relative low compared with that IUPAC (International

321   Union of Pure and Applied Chemistry) recommended on the surface of mineral dust

322   (0.013, 290-300K) (Crowley et al., 2010b) or determined in many field experiments

323   (e.g. S.S. Brown et al., 2006; 2009; Wagner et al., 2013; Morgan et al., 2015; Phillips

324   et al., 2016; Z. Wang et al., 2017; Brown et al., 2016; H.C. Wang et al., 2017b; X.F.

325   Wang et al., 2017), suggesting the particulate nitrate formation via N_2O_5 uptake was

326   easily maximized in polluted episode, and further worsen the PM pollution.

327   In the base case, the modeled particulate nitrate formation via N_2O_5 uptake is an

328   upper limit result, as the $ClNO_2$ yield set to zero. Since large coral combustion

329   emitted chloride into the atmosphere in the heating period in Beijing (Sun et al., 2013),

330   associated with the emission by power plants in North China. The enhanced

331   anthropogenic emission of chloride provides abundant chloride-containing aerosol to

332   form $ClNO_2$ via N_2O_5 uptake aloft, implying that significant $ClNO_2$ formed in the

333   upper layer of NBL (Tham et al., 2016; Z. Wang et al., 2017). Assuming the $ClNO_2$

334   yield is the average value of 0.28 determined at high altitude in North China (Z. Wang

335   et al., 2017), the produced pNO_3^- throughout the whole night will decreased 7 $\mu g\ m^{-3}$.

336   The $ClNO_2$ formation aloft throughout the night reach up to 2.5 ppbv, which is

337   comparable with that observed in the field measurement in North China (Tham et al.,

338   2016; Z. Wang et al., 2017; X.F. Wang et al., 2017). As the error of pNO_3^- formation

339   simulation was subject to the $ClNO_2$ yield, higher yield would increase the model

340   uncertainty directly, probing the $ClNO_2$ yield are warranted in future studies. As for

341   NO_3 reactivity, Figure 7 shows sensitivity tests of the integral pNO_3^- formation in the

342   whole night at k_{NO3} = 0.001 s^{-1}, 0.01 s^{-1}, 0.02 s^{-1}, 0.05 s^{-1}. The integral pNO_3^-

343   formation was decreased when k_{NO3} vary from 0.001 s^{-1} to 0.1 s^{-1}, but the variation

344   ratio to base case was within ±5%. The result shows the NO_3-N_2O_5 loss via NO_3 react

345   with VOCs in polluted wintertime is not important, which may only lead to relative

346   small uncertainties to the integral pNO_3^- formation calculation. Nevertheless, if N_2O_5

347   uptake was extremely low (e.g. $\gamma_{N2O5} < 10^{-4}$), the uncertainty cased by NO_3 oxidation

348   will be enlarged significantly.

349

4. Conclusion

351   During the wintertime, ambient O_3 is often fully titrated to be zero at the ground of

352   urban Beijing due to fast reaction with NO emissions. Consequently, the near surface

353   air masses were chemically inert. Nevertheless, the chemical information of the air

354   masses at higher altitudes was indicative of a reactive layer above urban Beijing,

355   which potentially drives fast pNO_3^- production via N_2O_5 uptake. In this study, we

356   evidenced of an additional Ox missing aloft with 25 ppb throughout the night. Based

357   on model simulation, we found the particulate nitrate formed above 150 m can reach

358   up to 50 $\mu g\ m^{-3}$, and enhance the surface level PM concentration significantly with 28

359   $\mu g\ m^{-3}$ after NBL breaking. Our study also demonstrated that during heavy PM

360   pollution period, the particulate nitrate formation capacity via N_2O_5 uptake is easily

361   maximized in the upper layer, even N_2O_5 uptake is as low as 1.7×10^{-3}, indicating the

362   mixing ratio of NO_2 aloft are directly linked to nitrate formation, and reduction of

363   NOx is helpful to decrease nocturnal nitrate formation. Overall, this study highlights

364   the importance of the interplay between chemical formation aloft and dynamic

365   processes for probing the ground level PM pollution problem. In the future, direct

366   observations of N_2O_5 and associated parameters should be performed to explore the

367   physical and chemical properties of this overhead nighttime reaction layer, and

368   reached a better understanding of the winter haze formation.

369

370   *Acknowledgements.*

371   This work was supported by the National Natural Science Foundation of China (Grant

372   No. 91544225, 41375124, 21522701 and 41571130021). The authors gratefully

373   acknowledge the science team of Peking University for their general support, as well

374   as the team running the tower platform, which enabled the vertical profile

375   observations.

376

References.

Baasandorj, M., Hoch, S. W., Bares, R., Lin, J. C., Brown, S. S., Millet, D. B., Martin, R., Kelly, K., Zarzana, K. J., Whiteman, C. D., Dube, W. P., Tonnesen, G., Jaramillo, I. C., and Sohl, J.: Coupling between Chemical and Meteorological Processes under Persistent Cold-Air Pool Conditions: Evolution of Wintertime $PM_{2.5}$ Pollution Events and N_2O_5 Observations in Utah's Salt Lake Valley, Environ Sci Technol, 51, 5941-5950, 2017.

Badger, C. L., Griffiths, P. T., George, I., Abbatt, J. P. D., and Cox, R. A.: Reactive uptake of N_2O_5 by aerosol particles containing mixtures of humic acid and ammonium sulfate, J Phys Chem A, 110, 6986-6994, 2006.

Benton, A. K., Langridge, J. M., Ball, S. M., Bloss, W. J., Dall'Osto, M., Nemitz, E., Harrison, R. M., and Jones, R. L.: Night-time chemistry above London: measurements of NO_3 and N_2O_5 from the BT Tower, Atmos Chem Phys, 10, 9781-9795, 2010.

Bertram, T. H., Thornton, J. A., and Riedel, T. P.: An experimental technique for the direct measurement of N_2O_5 reactivity on ambient particles, Atmos Meas Tech, 2, 231-242, 2009.

Brown, S. G., Roberts, P. T., McCarthy, M. C., Lurmann, F. W., and Hyslop, N. P.: Wintertime vertical variations in particulate matter (PM) and precursor concentrations in the San Joaquin Valley during the California Regional coarse PM/fine PM Air Quality Study, J Air Waste Manage, 56, 1267-1277, 2006.

Brown, S. S., Dube, W. P., Fuchs, H., Ryerson, T. B., Wollny, A. G., Brock, C. A., Bahreini, R., Middlebrook, A. M., Neuman, J. A., Atlas, E., Roberts, J. M., Osthoff, H. D., Trainer, M., Fehsenfeld, F. C., and Ravishankara, A. R.: Reactive uptake coefficients for N_2O_5 determined from aircraft measurements during the Second Texas Air Quality Study: Comparison to current model parameterizations, J Geophys Res-Atmos, 114, 2009.

Brown, S. S., Dube, W. P., Osthoff, H. D., Wolfe, D. E., Angevine, W. M., and Ravishankara, A. R.: High resolution vertical distributions of NO_3 and N_2O_5 through the nocturnal boundary layer, Atmos Chem Phys, 7, 139-149, 2007.

Brown, S. S., Dube, W. P., Tham, Y. J., Zha, Q. Z., Xue, L. K., Poon, S., Wang, Z., Blake, D. R., Tsui, W., Parrish, D. D., and Wang, T.: Nighttime chemistry at a high altitude site above Hong Kong, J Geophys Res-Atmos, 121, 2457-2475, 2016.

Brown, S. S., Ryerson, T. B., Wollny, A. G., Brock, C. A., Peltier, R., Sullivan, A. P., Weber, R. J., Dube, W. P., Trainer, M., Meagher, J. F., Fehsenfeld, F. C., and Ravishankara, A. R.: Variability in nocturnal nitrogen oxide processing and its role in regional air quality, Science, 311, 67-70, 2006.

Brown, S. S. and Stutz, J.: Nighttime radical observations and chemistry, Chem Soc Rev, 41, 6405-6447, 2012.

Cao, J. J., Xu, H. M., Xu, Q., Chen, B. H., and Kan, H. D.: Fine Particulate Matter Constituents and Cardiopulmonary Mortality in a Heavily Polluted Chinese City, Environ Health Persp, 120, 373-378, 2012.

Chan, C. Y., Xu, X. D., Li, Y. S., Wong, K. H., Ding, G. A., Chan, L. Y., and Cheng, X. H.: Characteristics of vertical profiles and sources of $PM_{2.5}$, PM_{10} and carbonaceous species in Beijing, Atmos Environ, 39, 5113-5124, 2005.

Chen, C., Sun, Y. L., Xu, W. Q., Du, W., Zhou, L. B., Han, T. T., Wang, Q. Q., Fu, P. Q., Wang, Z. F., Gao, Z. Q., Zhang, Q., and Worsnop, D. R.: Characteristics and sources of submicron aerosols above the urban canopy (260 m) in Beijing, China, during the 2014 APEC summit,

421   Atmos Chem Phys, 15, 12879-12895, 2015.

422   Crowley, J. N., Ammann, M., Cox, R. A., Hynes, R. G., Jenkin, M. E., Mellouki, A., Rossi, M. J.,
423   Troe, J., and Wallington, T. J.: Evaluated kinetic and photochemical data for atmospheric
424   chemistry: Volume V - heterogeneous reactions on solid substrates, Atmos Chem Phys, 10,
425   9059-9223, 2010b.

426   Crowley, J. N., Schuster, G., Pouvesle, N., Parchatka, U., Fischer, H., Bonn, B., Bingemer, H., and
427   Lelieveld, J.: Nocturnal nitrogen oxides at a rural mountain-site in south-western Germany,
428   Atmos Chem Phys, 10, 2795-2812, 2010a.

429   Ferrero, L., Cappelletti, D., Moroni, B., Sangiorgi, G., Perrone, M. G., Crocchianti, S., and
430   Bolzacchini, E.: Wintertime aerosol dynamics and chemical composition across the mixing
431   layer over basin valleys, Atmos Environ, 56, 143-153, 2012.

432   Ferrero, L., Perrone, M. G., Petracone, S., Sangiorgi, G., Ferrini, B. S., Lo Porto, C., Lazzati, Z.,
433   Cocchi, D., Bruno, F., Greco, F., Riccio, A., and Bolzacchini, E.: Vertically-resolved particle
434   size distribution within and above the mixing layer over the Milan metropolitan area, Atmos
435   Chem Phys, 10, 3915-3932, 2010.

436   Gross, S. and Bertram, A. K.: Reactive uptake of NO_3, N_2O_5, NO_2, HNO_3, and O_3 on three types
437   of polycyclic aromatic hydrocarbon surfaces, J Phys Chem A, 112, 3104-3113, 2008.

438   Gross, S., Iannone, R., Xiao, S., and Bertram, A. K.: Reactive uptake studies of NO_3 and N_2O_5 on
439   alkenoic acid, alkanoate, and polyalcohol substrates to probe nighttime aerosol chemistry,
440   Phys Chem Chem Phys, 11, 7792-7803, 2009.

441   Grzinic, G., Bartels-Rausch, T., Berkemeier, T., Turler, A., and Ammann, M.: Viscosity controls
442   humidity dependence of N2O5 uptake to citric acid aerosol, Atmos Chem Phys, 15,
443   13615-13625, 2015.

444   Guo, S., Hu, M., Zamora, M. L., Peng, J. F., Shang, D. J., Zheng, J., Du, Z. F., Wu, Z., Shao, M.,
445   Zeng, L. M., Molina, M. J., and Zhang, R. Y.: Elucidating severe urban haze formation in
446   China, P Natl Acad Sci USA, 111, 17373-17378, 2014.

447   Hallquist, M., Stewart, D. J., Stephenson, S. K., and Cox, R. A.: Hydrolysis of N_2O_5 on
448   sub-micron sulfate aerosols, Phys Chem Chem Phys, 5, 3453-3463, 2003.

449   Huang, R. J., Zhang, Y. L., Bozzetti, C., Ho, K. F., Cao, J. J., Han, Y. M., Daellenbach, K. R.,
450   Slowik, J. G., Platt, S. M., Canonaco, F., Zotter, P., Wolf, R., Pieber, S. M., Bruns, E. A.,
451   Crippa, M., Ciarelli, G., Piazzalunga, A., Schwikowski, M., Abbaszade, G., Schnelle-Kreis, J.,
452   Zimmermann, R., An, Z. S., Szidat, S., Baltensperger, U., El Haddad, I., and Prevot, A. S. H.:
453   High secondary aerosol contribution to particulate pollution during haze events in China,
454   Nature, 514, 218-222, 2014.

455   Kane, S. M., Caloz, F., and Leu, M. T.: Heterogeneous uptake of gaseous N_2O_5 by $(NH_4)^2SO_4$,
456   NH_4HSO_4, and H_2SO_4 aerosols, J Phys Chem A, 105, 6465-6470, 2001.

457   Kim, Y. J., Spak, S. N., Carmichael, G. R., Riemer, N., and Stanier, C. O.: Modeled aerosol nitrate
458   formation pathways during wintertime in the Great Lakes region of North America, J
459   Geophys Res-Atmos, 119, 12420-12445, 2014.

460   Lei, H. and Wuebbles, D. J.: Chemical competition in nitrate and sulfate formations and its effect
461   on air quality, Atmos Environ, 80, 472-477, 2013.

462   Lurmann, F. W., Brown, S. G., McCarthy, M. C., and Roberts, P. T.: Processes influencing
463   secondary aerosol formation in the San Joaquin Valley during winter, J Air Waste Manage, 56,
464   1679-1693, 2006.

465   Mentel, T. F., Sohn, M., and Wahner, A.: Nitrate effect in the heterogeneous hydrolysis of
466   dinitrogen pentoxide on aqueous aerosols, Phys Chem Chem Phys, 1, 5451-5457, 1999.
467   Morgan, W. T., Ouyang, B., Allan, J. D., Aruffo, E., Di Carlo, P., Kennedy, O. J., Lowe, D., Flynn,
468   M. J., Rosenberg, P. D., Williams, P. I., Jones, R., McFiggans, G. B., and Coe, H.: Influence
469   of aerosol chemical composition on N_2O_5 uptake: airborne regional measurements in
470   northwestern Europe, Atmos Chem Phys, 15, 973-990, 2015.
471   Pathak, R. K., Wang, T., and Wu, W. S.: Nighttime enhancement of $PM_{2.5}$ nitrate in ammonia-poor
472   atmospheric conditions in Beijing and Shanghai: Plausible contributions of heterogeneous
473   hydrolysis of N2O5 and HNO3 partitioning, Atmos Environ, 45, 1183-1191, 2011.
474   Pathak, R. K., Wu, W. S., and Wang, T.: Summertime $PM_{2.5}$ ionic species in four major cities of
475   China: nitrate formation in an ammonia-deficient atmosphere, Atmos Chem Phys, 9,
476   1711-1722, 2009.
477   Phillips, G. J., Thieser, J., Tang, M. J., Sobanski, N., Schuster, G., Fachinger, J., Drewnick, F.,
478   Borrmann, S., Bingemer, H., Lelieveld, J., and Crowley, J. N.: Estimating N_2O_5 uptake
479   coefficients using ambient measurements of NO_3, N_2O_5, $ClNO_2$ and particle-phase nitrate,
480   Atmos Chem Phys, 16, 13231-13249, 2016.
481   Pusede, S. E., Duffey, K. C., Shusterman, A. A., Saleh, A., Laughner, J. L., Wooldridge, P. J.,
482   Zhang, Q., Parworth, C. L., Kim, H., Capps, S. L., Valin, L. C., Cappa, C. D., Fried, A.,
483   Walega, J., Nowak, J. B., Weinheimer, A. J., Hoff, R. M., Berkoff, T. A., Beyersdorf, A. J.,
484   Olson, J., Crawford, J. H., and Cohen, R. C.: On the effectiveness of nitrogen oxide
485   reductions as a control over ammonium nitrate aerosol, Atmos Chem Phys, 16, 2575-2596,
486   2016.
487   Riedel, T. P., Wagner, N. L., Dube, W. P., Middlebrook, A. M., Young, C. J., Ozturk, F., Bahreini,
488   R., VandenBoer, T. C., Wolfe, D. E., Williams, E. J., Roberts, J. M., Brown, S. S., and
489   Thornton, J. A.: Chlorine activation within urban or power plant plumes: Vertically resolved
490             $ClNO_2$ and Cl_2 measurements from a tall tower in a polluted continental setting, J Geophys
491   Res-Atmos, 118, 8702-8715, 2013.
492   Sander, S. P., et al. (2011), Chemical Kinetics and Photochemical Data for Use in Atmospheric
493   Studies Evaluation Number 17, JPL Publication 10–6 Rep., NASA Jet Propul. Lab, Pasadena,
494   California.
495   Seinfeld, J. H., Pandis, S.N., (2006). Atmospheric Chemistry and Physics: from Air Pollution to
496   Climate Change (Second edition), John Wiley & Sons, Inc., Hoboken, New Jersey.
497   Stutz, J., Wong, K. W., Lawrence, L., Ziemba, L., Flynn, J. H., Rappenglück, B., and Lefer, B.:
498   Nocturnal NO_3 radical chemistry in Houston, TX, Atmos Environ, 44, 4099-4106, 2010.
499   Su, X., Tie, X. X., Li, G. H., Cao, J. J., Huang, R. J., Feng, T., Long, X., and Xu, R. G.: Effect of
500   hydrolysis of N_2O_5 on nitrate and ammonium formation in Beijing China: WRF-Chem model
501   simulation, Sci Total Environ, 579, 221-229, 2017.
502   Sun, Y. L., Du, W., Wan, Q. Q., Zhang, Q., Chen, C., Chen, Y., Chen, Z. Y., Fu, P. Q., Wang, Z. F.,
503   Gao, Z. Q., and Worsnop, D. R.: Real-Time Characterization of Aerosol Particle Composition
504   above the Urban Canopy in Beijing: Insights into the Interactions between the Atmospheric
505   Boundary Layer and Aerosol Chemistry, Environ Sci Technol, 49, 11340-11347, 2015b.
506   Sun, Y. L., Wang, Z. F., Du, W., Zhang, Q., Wang, Q. Q., Fu, P. Q., Pan, X. L., Li, J., Jayne, J., and
507   Worsnop, D. R.: Long-term real-time measurements of aerosol particle composition in
508   Beijing, China: seasonal variations, meteorological effects, and source analysis, Atmos Chem

509   Phys, 15, 10149-10165, 2015a.

510 Sun, Y. L., Wang, Z. F., Fu, P. Q., Yang, T., Jiang, Q., Dong, H. B., Li, J., and Jia, J. J.: Aerosol
511   composition, sources and processes during wintertime in Beijing, China, Atmos Chem Phys,
512   13, 4577-4592, 2013.

513 Tham, Y. J., Wang, Z., Li, Q. Y., Yun, H., Wang, W. H., Wang, X. F., Xue, L. K., Lu, K. D., Ma, N.,
514   Bohn, B., Li, X., Kecorius, S., Gross, J., Shao, M., Wiedensohler, A., Zhang, Y. H., and Wang,
515   T.: Significant concentrations of nitryl chloride sustained in the morning: investigations of
516   the causes and impacts on ozone production in a polluted region of northern China, Atmos
517   Chem Phys, 16, 14959-14977, 2016.

518 Thornton, J. A., Braban, C. F., and Abbatt, J. P. D.: N_2O_5 hydrolysis on sub-micron organic
519   aerosols: the effect of relative humidity, particle phase, and particle size, Phys Chem Chem
520   Phys, 5, 4593-4603, 2003.

521 Thornton, J. A., Kercher, J. P., Riedel, T. P., Wagner, N. L., Cozic, J., Holloway, J. S., Dube, W. P.,
522   Wolfe, G. M., Quinn, P. K., Middlebrook, A. M., Alexander, B., and Brown, S. S.: A large
523   atomic chlorine source inferred from mid-continental reactive nitrogen chemistry, Nature,
524   464, 271-274, 2010.

525 Tsai, C., Wong, C., Hurlock, S., Pikelnaya, O., Mielke, L. H., Osthoff, H. D., Flynn, J. H., Haman,
526   C., Lefer, B., Gilman, J., de Gouw, J., and Stutz, J.: Nocturnal loss of NOx during the 2010
527   CalNex-LA study in the Los Angeles Basin, J Geophys Res-Atmos, 119, 13004-13025, 2014.

528 Wagner, N. L., Riedel, T. P., Young, C. J., Bahreini, R., Brock, C. A., Dube, W. P., Kim, S.,
529   Middlebrook, A. M., Ozturk, F., Roberts, J. M., Russo, R., Sive, B., Swarthout, R., Thornton,
530   J. A., VandenBoer, T. C., Zhou, Y., and Brown, S. S.: N_2O_5 uptake coefficients and nocturnal
531   NO_2 removal rates determined from ambient wintertime measurements, J Geophys
532   Res-Atmos, 118, 9331-9350, 2013.

533 Wahner, A., Mentel, T. F., and Sohn, M.: Gas-phase reaction of N_2O_5 with water vapor:
534   Importance of heterogeneous hydrolysis of N_2O_5 and surface desorption of HNO_3 in a large
535   teflon chamber, Geophys Res Lett, 25, 2169-2172, 1998.

536 Wang, H. C. and Lu, K. D.: Determination and Parameterization of the Heterogeneous Uptake
537   Coefficient of Dinitrogen Pentoxide (N_2O_5), Prog Chem, 28, 917-933, 2016.

538 Wang, H. C., Lu, K. D., Chen, X. R., Zhu, Q. D., Chen, Q., Guo, S., Jiang, M. Q., Li, X., Shang, D.
539   J., Tan, Z. F., Wu, Y. S., Wu, Z. J., Zou, Q., Zheng, Y., Zeng, L. M., Zhu, T., Hu, M., and
540   Zhang, Y. H.: High N_2O_5 Concentrations Observed in Urban Beijing: Implications of a Large
541   Nitrate Formation Pathway, Environ Sci Tech Let, 4, 416-420, 2017b.

542 Wang, H. C., Lu, K. D., Tan, Z. F., Sun, K., Li, X., Hu, M., Shao, M., Zeng, L. M., Zhu, T., and
543   Zhang, Y. H.: Model simulation of NO_3, N_2O_5 and $ClNO_2$ at a rural site in Beijing during
544   CAREBeijing-2006, Atmos Res, 196, 97-107, 2017a.

545 Wang, X. F., Wang, H., Xue, L. K., Wang, T., Wang, L. W., Gu, R. R., Wang, W. H., Tham, Y. J.,
546   Wang, Z., Yang, L. X., Chen, J. M., and Wang, W. X.: Observations of N_2O_5 and $ClNO_2$ at a
547   polluted urban surface site in North China: High N_2O_5 uptake coefficients and low $ClNO_2$
548   product yields, Atmos Environ, 156, 125-134, 2017.

549 Wang, Z., Wang, W. H., Tham, Y. J., Li, Q. Y., Wang, H., Wen, L., Wang, X. F., and Wang, T.: Fast
550   heterogeneous N_2O_5 uptake and $ClNO_2$ production in power plant and industrial plumes
551   observed in the nocturnal residual layer over the North China Plain, Atmos Chem Phys, 17,
552   12361-12378, 2017.

553 Watson, J. G. and Chow, J. C.: A wintertime $PM_{2.5}$ episode at the fresno, CA, supersite, Atmos
554   Environ, 36, 465-475, 2002.
555 Wen, L. A., Chen, J. M., Yang, L. X., Wang, X. F., Xu, C. H., Sui, X. A., Yao, L., Zhu, Y. H.,
556   Zhang, J. M., Zhu, T., and Wang, W. X.: Enhanced formation of fine particulate nitrate at a
557   rural site on the North China Plain in summer: The important roles of ammonia and ozone,
558   Atmos Environ, 101, 294-302, 2015.
559 Ying, Q.: Physical and chemical processes of wintertime secondary nitrate aerosol formation,
560   Front Environ Sci En, 5, 348-361, 2011.
561 Zhang, Q., Jimenez, J. L., Canagaratna, M. R., Allan, J. D., Coe, H., Ulbrich, I., Alfarra, M. R.,
562   Takami, A., Middlebrook, A. M., Sun, Y. L., Dzepina, K., Dunlea, E., Docherty, K., DeCarlo,
563   P. F., Salcedo, D., Onasch, T., Jayne, J. T., Miyoshi, T., Shimono, A., Hatakeyama, S.,
564   Takegawa, N., Kondo, Y., Schneider, J., Drewnick, F., Borrmann, S., Weimer, S., Demerjian,
565   K., Williams, P., Bower, K., Bahreini, R., Cottrell, L., Griffin, R. J., Rautiainen, J., Sun, J. Y.,
566   Zhang, Y. M., and Worsnop, D. R.: Ubiquity and dominance of oxygenated species in organic
567   aerosols in anthropogenically-influenced Northern Hemisphere midlatitudes, Geophys Res
568   Lett, 34, 2007.
569 Zhang, R. Y., Wang, G. H., Guo, S., Zarnora, M. L., Ying, Q., Lin, Y., Wang, W. G., Hu, M., and
570   Wang, Y.: Formation of Urban Fine Particulate Matter, Chem Rev, 115, 3803-3855, 2015.
571 Zheng, G. J., Duan, F. K., Su, H., Ma, Y. L., Cheng, Y., Zheng, B., Zhang, Q., Huang, T., Kimoto,
572   T., Chang, D., Poschl, U., Cheng, Y. F., and He, K. B.: Exploring the severe winter haze in
573   Beijing: the impact of synoptic weather, regional transport and heterogeneous reactions,
574   Atmos Chem Phys, 15, 2969-2983, 2015.
575 Zhong, J. T., Zhang, X. Y., Wang, Y. Q., Sun, J. Y., Zhang, Y. M., Wang, J. Z., Tan, K. Y., Shen,
576   X. J., Che, H. C., Zhang, L., Zhang, Z. X., Qi, X. F., Zhao, H. R., Ren, S. X., and Li, Y.:
577   Relative Contributions of Boundary-Layer Meteorological Factors to the Explosive Growth
578   of $PM_{2.5}$ during the Red-Alert Heavy Pollution Episodes in Beijing in December 2016, J
579   Meteorol Res-Prc, 31, 809-819, 2017.

580
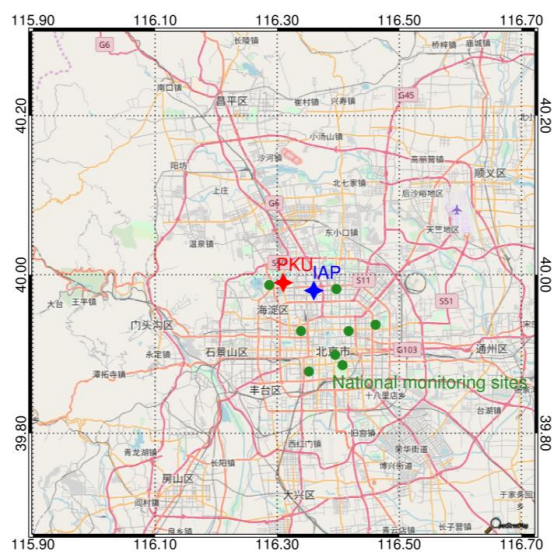
Figure 1. Location of the monitoring sites used in this study, including PKU (red diamond), IAP (blue diamond), and other National Monitoring Sites (green circles). Vertical profiles of NOx and O_3 were collected at a tower at the IAP. Measurements of particle number and size distribution (used to calculate N_2O_5 and particle nitrate formation) were collected from a ground site at PKU. Additional measurements on $PM_{2.5}$ concentrations were continuously measured at national monitoring sites throughout Beijing.

588

589
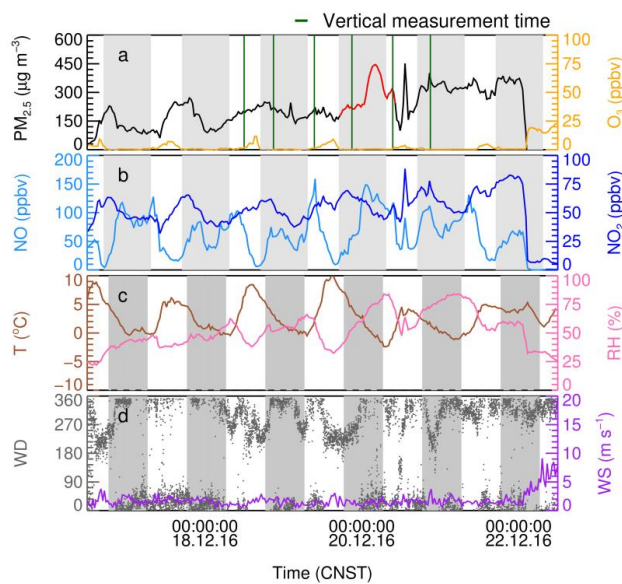
Figure 2. Time series of **(a)** PM$_{2.5}$ and O$_3$, **(b)** NO and NO$_2$, **(c)** temperature (T) and relative humidity (RH), **(d)** wind direction (WD) and wind speed (WS) from December 16 to 22, 2016 (CNST, Chinese National Standard Time) at PKU site in Beijing, China. The shaded region represents the nighttime periods. Red line in panel **(a)** shows an example of fast PM$_{2.5}$ enhancement on the night of December 19, and the green lines are the time periods when the vertical measurements conducted in IAP site.
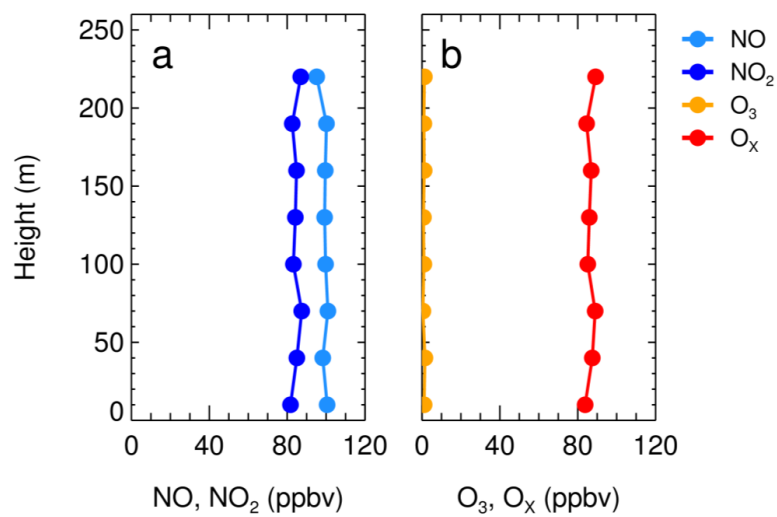
Figure 3. Vertical profiles of NO and NO_2 (**a**), O_3 and Ox (**b**) at 20:38-21:06 on the night of December 20, 2016.

601
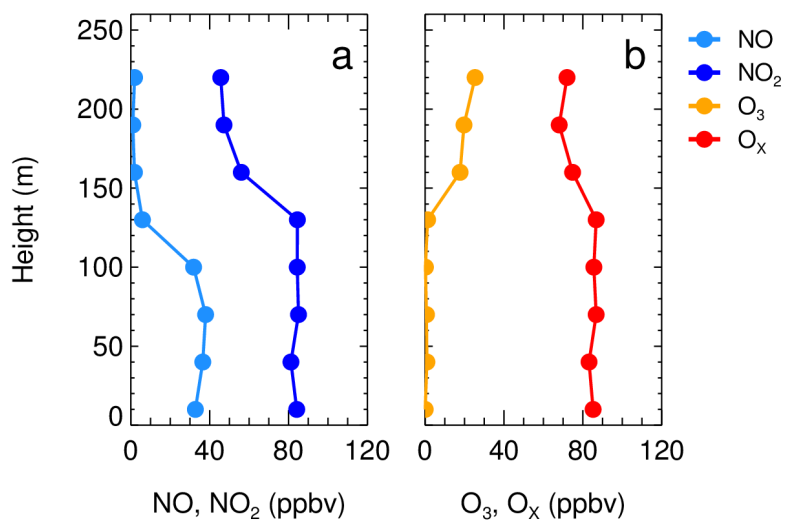
Figure 4. O_X missing case presented by the vertical profiles of (**a**) NO and NO_2, (**b**)
O_3 and O_X at 20:38-21:13 on the night of December 19, 2016.

604

605
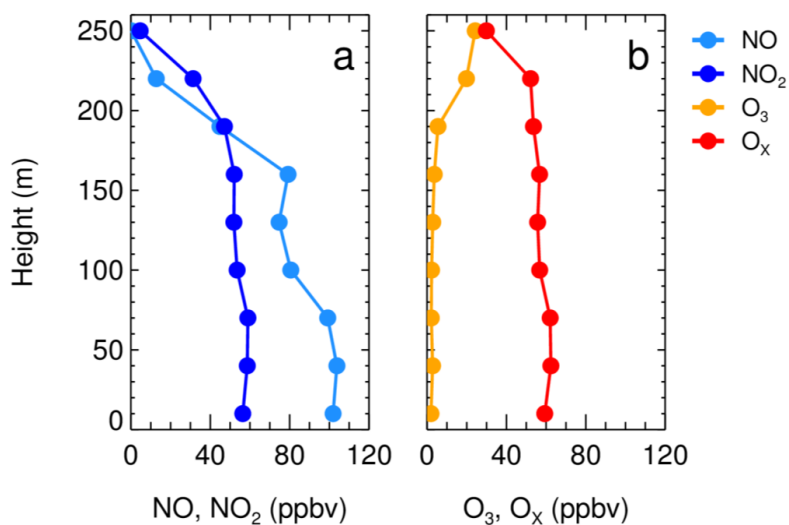
Figure 5. Vertical profiles of (**a**) NO and NO$_2$, (**b**) O$_3$ and O$_X$ at 09:06-09:34 in the
morning of December 20, 2016.

608

609

610
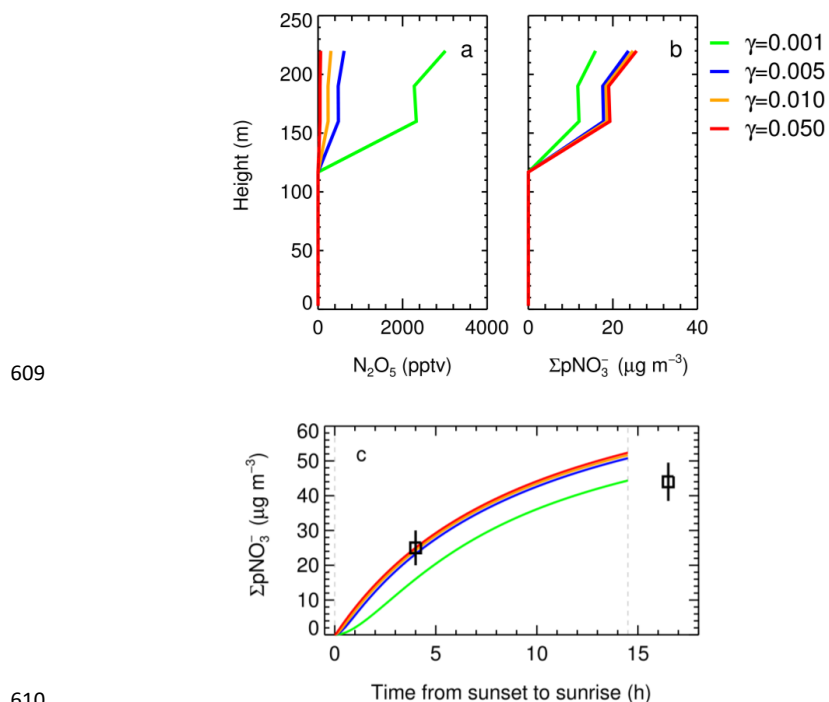
Figure 6. Base case (γ=0.005) and sensitivity tests of the vertical profile on the night
of December 19 at different N_2O_5 uptake coefficients, including **(a)** the mixing ratio
of N_2O_5 at 21:00, **(b)** the integral pNO_3^- production from sunset to 21:00, **(c)** the time
series of the integral pNO_3^- formed at 240 m via N_2O_5 uptake from sunset (17:00) to
sunrise (07:30, nighttime length = 14.5 h), the squares represents the pNO_3^- equivalent
weight from the observed O_X missing in the two vertical measurements ~21:00 and
~09:30 in the following morning.

618
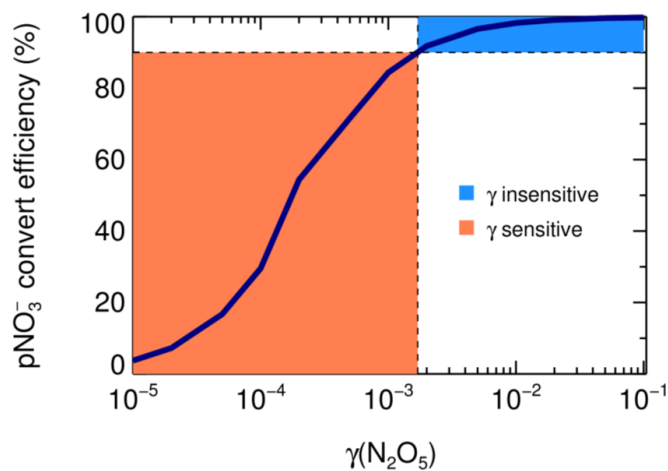
Figure 7. The dependence of pNO$_3^-$ convert efficiency by N$_2$O$_5$ uptake on γ_{N2O5}. The initial S_a set to 3000 μm^2 cm^{-3}, the ClNO$_2$ yield is zero and k$_{NO3}$ is 0.02 s^{-1}. The orange region shows the convert efficiency is sensitive when $\gamma < 0.0017$, while the blue region shows the convert efficiency is over 90% and insensitive when $\gamma \geq 0.0017$.
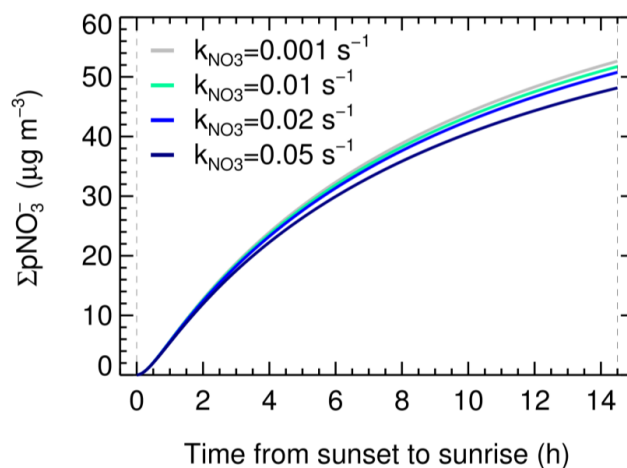
Figure 8. Base case (k_{NO3}=0.02 s^{-1}) and sensitivity tests of the integral pNO$_3^-$ formed at 240 m via N$_2$O$_5$ uptake at different NO$_3$ reactivity (0.001 s^{-1}, 0.01 s^{-1}, 0.05 s^{-1}) on the whole night of December 19, 2016.

630   **Table 1.** List of the parameter sets in base case and sensitivity tests.

Cases	k_{NO3} (s^{-1})	γ_{N2O5}
Base case	0.02	0.005
k_{NO3} test 1	0.001	0.005
k_{NO3} test 2	0.01	0.005
k_{NO3} test 3	0.05	0.005
γ_{N2O5} test 1	0.02	0.001
γ_{N2O5} test 2	0.02	0.01
γ_{N2O5} test 3	0.02	0.05

631